

# Dynamic Behavior of Molecular Switches in Crystal under Pressure and Its Reflection on Tactile Sensing

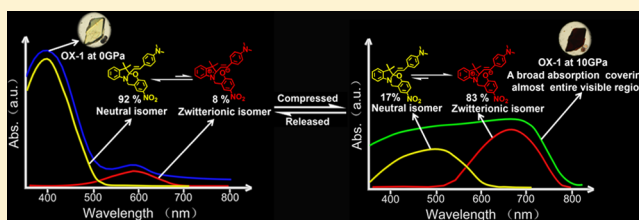
Yi Wang,<sup>†</sup> Xiao Tan,<sup>‡</sup> Yu-Mo Zhang,<sup>†</sup> Shaoyin Zhu,<sup>†</sup> Ivan Zhang,<sup>†</sup> Binhong Yu,<sup>†</sup> Kai Wang,<sup>‡</sup> Bing Yang,<sup>†</sup> Minjie Li,<sup>\*,†</sup> Bo Zou,<sup>\*,‡</sup> and Sean Xiao-An Zhang<sup>\*,†</sup>

<sup>†</sup>State Key Laboratory of Supramolecular Structure and Materials, Jilin University, Changchun, Jilin 130012, China

<sup>‡</sup>State Key Laboratory of Superhard Materials, Jilin University, Changchun, Jilin 130012, China

## S Supporting Information

**ABSTRACT:** Molecular switches have attracted increasing interest in the past decades, due to their broad applications in data storage, optical gating, smart windows, and so on. However, up till now, most of the molecular switches are operated in solutions or polymer blends with the stimuli of light, heat, and electric fields. Herein, we demonstrate the first pressure-controllable molecular switch of a benzo[1,3]oxazine OX-1 in crystal. Distinct from the light-triggered tautomerization between two optical states, applying hydrostatic pressure on the OX-1 crystal results in large-scale and continuous states across the whole visible light range (from ~430 to ~700 nm), which has not been achieved with other stimuli. Based on detailed and systematic control experiments and theoretical calculation, the preliminary requirements and mechanism of pressure-dependent tautomerization are fully discussed. The contributions of molecular tautomerization to the large-scale optical modulation are also stressed. Finally, the importance of studying pressure-responsive materials on understanding tactile sensing is also discussed and a possible mechanotransduction mode is proposed.



## INTRODUCTION

Reversible molecular transformations are of paramount importance in many biological and chemical processes.<sup>1</sup> Various molecular tautomeric switches, such as spiropyrans, azobenzenes, and diarylethenes, have been hotly investigated to help understand the function-switching process in biological field, and also explore their broad applications in data storage, optical gating, smart windows, and so on.<sup>2–9</sup> Up till now, many stimuli (such as light, heat, and electric field) have already been demonstrated to be able to switch these molecular switches, but most of these studies are concentrated on their tautomerization between the bistable states in solution or in polymer blends<sup>10–16</sup> and limited examples show tunable tautomerization in constraint crystal states.<sup>17–19</sup> Pressure is a very common energy input in chemistry, but it has been rarely used to tune the tautomerization of molecular switches. Though some scattered examples (e.g., piroxicam) show pressure-induced tautomerization in solid state,<sup>20</sup> pressure-responsive tautomeric molecular switches have not attracted enough attention so far.

Quite different from other stimuli (such as light and heat) that can be directly absorbed by single molecule and trigger the tautomerization, the application and propagation of pressure are through the intermolecular interactions in condensed states.<sup>21–25</sup> Therefore, several fundamental and technological breakthroughs would be envisioned if the pressure could be used as a switching stimulus. First, the switching could be achieved in the crystal state, which is very hard to realize with other stimuli. Second, the two tautomeric states should be modified to generate more diversified states by the gradually enhanced intermolecular

interactions under increasing pressure. And some new application potentials for molecular switches could be expected. Last but not least, the relationship between pressure and molecular tautomerization would be established and it will shine light on the longtime unresolved problem on how mechanotransduction is triggered in the tactile nerve. Therefore, investigating the switching behavior of molecular switches under pressure is highly important.

Herein, we demonstrate for the first time that the tautomerization of a benzo[1,3]oxazine OX-1 (Figure 1) can be quantitatively tuned with the only parameter of hydrostatic pressure in the crystal state, which results in remarkable and continuous optical modulation that covers nearly the entire visible light range (from ~430 to ~700 nm). Such a large-scale and consecutive absorption modulation has not been achieved with other methods. And this tautomerization is strictly pressure-dependent with good reversibility. By comparing with the two control molecules, OX-2 and IA-1, it is revealed that (i) the low tautomerization energy barrier is a preliminary requirement for pressure-controllable tautomerization of molecular switches, (ii) difference in the compressibility of the two tautomeric species is the inherent cause of pressure-tunable tautomerization, and (iii) molecular structural tautomerization contributes more to such a large-scale optical modulation than the configuration changes. The new pressure-dependent switching behavior will exhibit new applications, as an example, OX-1 is used as a good candidate for

Received: November 8, 2014

Published: December 22, 2014

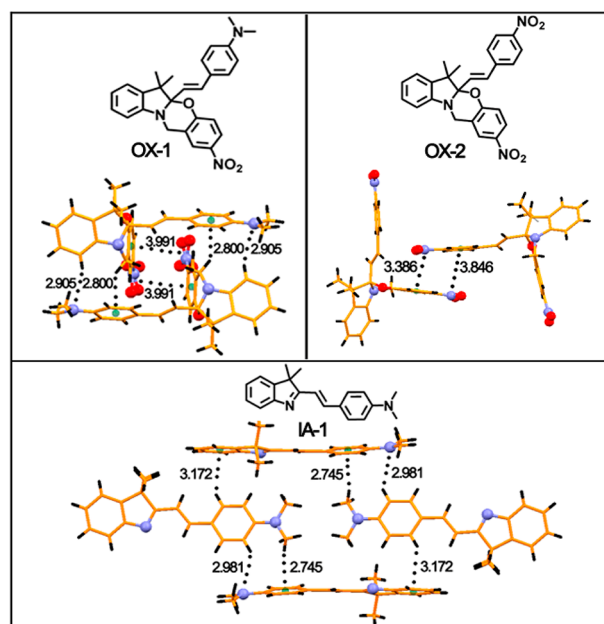


**Figure 1.** Chemical structures and partial view of the crystal packing of **OX-1**, **OX-2**, and **IA-1**. In the molecular skeleton, the black and orange regions represent hydrogen and carbon atoms, respectively. Red, blue, and green balls correspond to oxygen atoms, nitrogen atoms, and the center of an aromatic ring, respectively. The black dotted lines indicate various intermolecular interactions ( $C-H\cdots\pi$ ,  $C-H\cdots N$ , and  $\pi\cdots\pi$  interactions).

a visible colorimetric pressure sensor. In addition, this successful pressure-responsive molecular switch also helps understand how the tactile signals are generated in biological system, and a possible mechanotransduction mode has been proposed.

## RESULTS AND DISCUSSION

**Switching Behavior of OX-1 and OX-2 in Solution and Crystal States under Ambient Pressure.** Benzo[1,3]-oxazines are newly discovered bistable molecular switches in 2005.<sup>26</sup> Though they are structurally similar to the traditional well-known spiropyrans, they exhibit improved switching speed and stability owing to noninvolving of cis–trans transition and the absence of high energy-state conjugated zwitterions during the tautomerization (Figure 2a).<sup>27–31</sup> Thus, benzo[1,3]oxazines are expected to tautomerize in crystal more easily. Two benzo[1,3]oxazine derivatives of **OX-1**<sup>32–37</sup> and **OX-2** with the same backbone but distinctively different properties were selected for study. First, their switching behavior was studied in solution. Both **OX-1** and **OX-2** exhibit the light-triggered neutral-to-zwitterionic tautomerization in solution. The neutral ring-closed isomers of **OX-1** and **OX-2** are colorless in dichloromethane, and resultant zwitterionic ring-open isomers exhibit a purple color and a pale yellow color, respectively (Figure 2b and c). Besides the photochromic properties, it is found that their tautomerization happens dynamically in solution at room temperature from temperature-dependent NMR analysis (Supporting Information Figure S1). However, **OX-1** has much lower energy barrier ( $\Delta G = 11.51 \text{ kcal}\cdot\text{mol}^{-1}$ ) and higher rate constant ( $2.5 \times 10^4 \text{ s}^{-1}$ ) for ring-opening reaction than those of **OX-2** ( $16.86 \text{ kcal}\cdot\text{mol}^{-1}$ ,  $2 \text{ s}^{-1}$ ) (Supporting Information Table S1). As a result, the tautomerization of **OX-1** is highly dependent on the solution environment. In less-polar solvents, the neutral isomers dominate, and in high polar

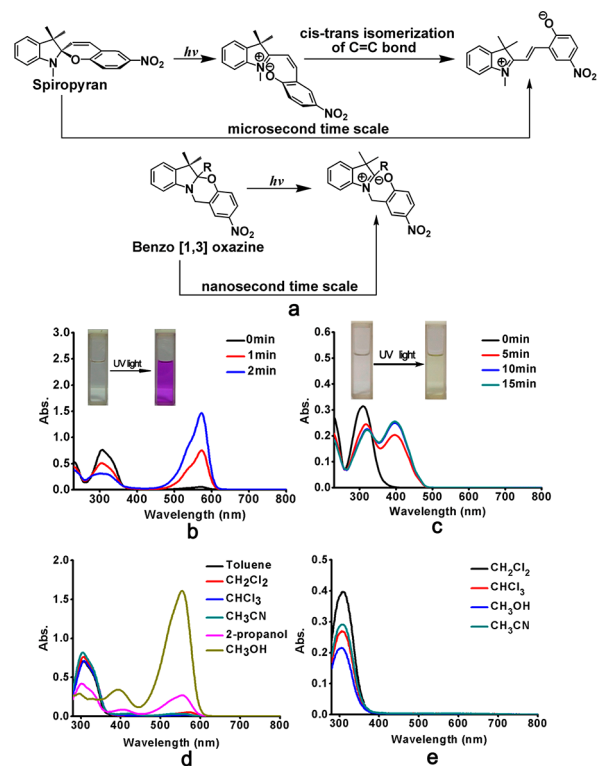


**Figure 2.** Comparison of the photoswitchable tautomerization between spiropyrans and benzo[1,3]oxazines (a); absorption spectra of **OX-1** (b) and **OX-2** (c) in dichloromethane solution ( $1 \times 10^{-5} \text{ M}$ ) under UV (254 nm 6W) irradiation for different times; absorption spectra of **OX-1** (d) and **OX-2** (e) in different solvents ( $1 \times 10^{-5} \text{ M}$ ) without the external light stimuli.

solvents, the zwitterionic isomers dominate without the external stimulus of light (Figure 2d). However, **OX-2** only exists in neutral ring-closed isomer in various test solvents (Figure 2e). This is presumably because the strong electron-donating *N,N*-dimethylamino group in **OX-1** can stabilize the positive charge in its zwitterionic isomer well, whereas the strong electron-withdrawing nitro group in **OX-2** makes the conjugated positive charge less stable.

After the study on tautomeric behavior of **OX-1** and **OX-2** in solutions, we tried to study their switching behavior in crystals. The single crystals of **OX-1** and **OX-2** were obtained by slow solvent evaporation, and their crystal structures are depicted in Figure 1 and Supporting Information Table S2. For the **OX-1** crystal, there is a very weak absorption sideband between 500 and 600 nm besides the main peak around 430 nm (black line in Figure 3b), and it is pale yellow in color (Figure 3a). Because the pale yellow color is uniformly distributed in the whole crystal, we can exclude the anomalous contamination of a small amount of purple zwitterionic isomers during the crystallization. Therefore, it is suggested that there are neutral and zwitterionic isomers coexisting in the crystal. To prove it, light irradiation (high pressure mercury lamp, 500 W) was used to shift the tautomerization equilibrium. As a result, the absorbance at 500–600 nm increased and their color turned to red from yellow (Supporting Information Figure S3a), which confirms that the sideband absorption is from the zwitterionic isomers and dynamic switching of **OX-1** surely exists in the crystal. Also, this is the first demonstration that tautomerization of certain molecular switch of benzo[1,3]oxazine can exist in crystal at room temperature without applying the conventional light

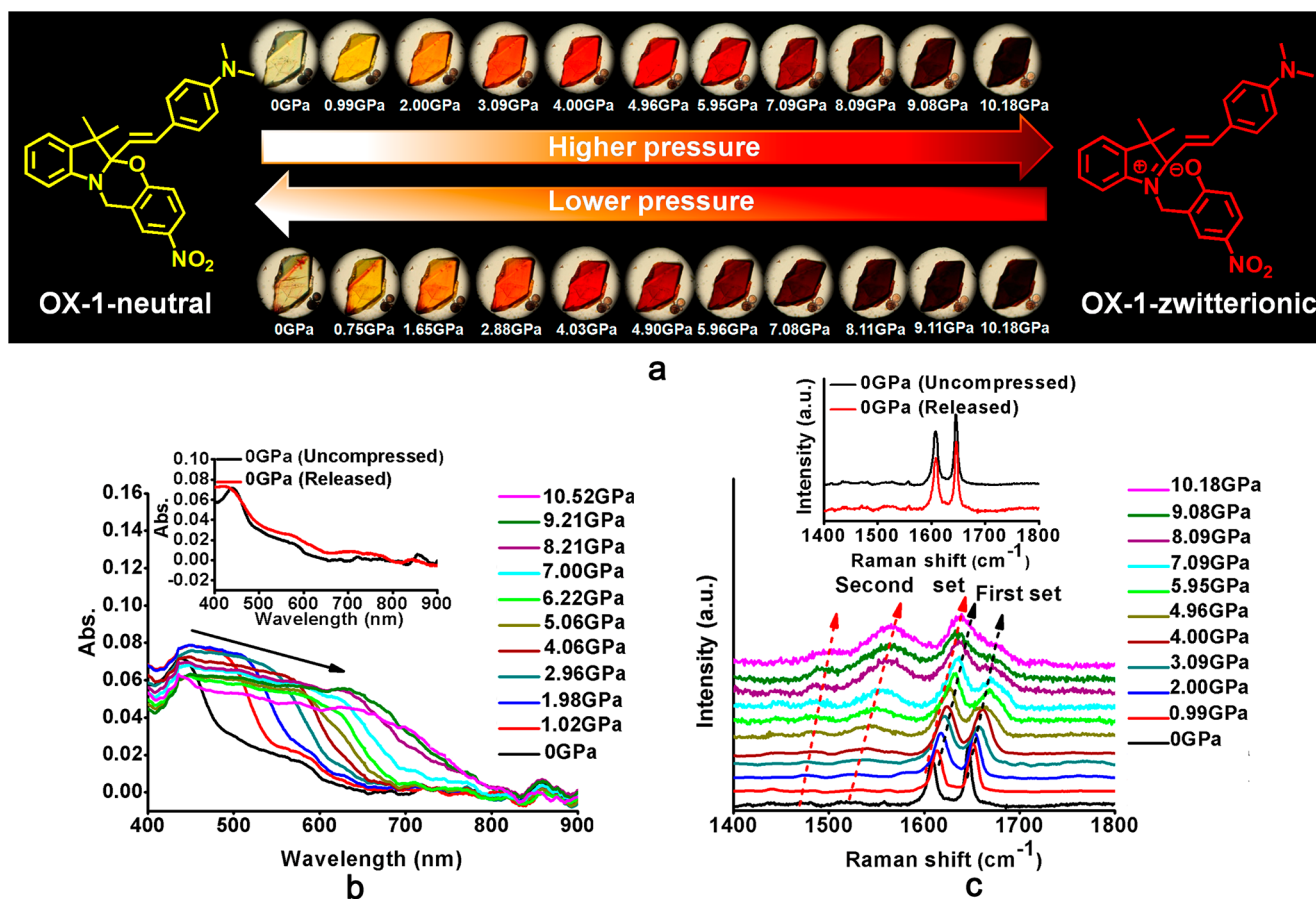


**Figure 3.** Molecular structure of OX-1 in neutral and zwitterionic forms, and real optical images of an OX-1 crystal with increasing and decreasing pressure (a) (the balls at the bottom right corner in DAC are ruby pressure markers). In-situ absorption (b) and Raman (c) spectra of the OX-1 crystal in the DAC with increasing pressure (inset: comparison of the absorption and Raman spectra of OX-1 in the uncompressed and released states).

stimulus. The reasons for the room-temperature tautomerization in constrained crystals are closely related to the low tautomeric energy barrier and small configurational change after tautomerization as we addressed before. Because the neutral isomers have lower energy than the zwitterionic isomers (Supporting Information Figure S4), neutral isomers dominate in the crystal (92% of OX-1 takes neutral forms in crystal roughly from UV-vis absorption spectra analysis) (Supporting Information Figure S6). As a result, only isomers in neutral form are detected in single crystal X-ray analysis (Figure 1 and Supporting Information Table S2).

In contrast, for OX-2, its crystal is colorless and transparent (Figure 4a), and the corresponding absorption spectrum shows only the absorption band for neutral isomers before 400 nm (black line in Figure 4b). Accordingly, single crystal X-ray structure analysis shows that there are only neutral isomers under ambient pressure. Under UV light (high pressure mercury lamp, 500 W) irradiation, the colorless OX-2 microcrystals turned to yellow with the appearance of absorption sideband in the visible light range (Supporting Information Figure S3b), which indicates that light stimulus can also induce the neutral-to-zwitterionic tautomerization of OX-2 in crystal. This marvelous light-triggered tautomerization phenomenon of OX-1 and OX-2 in crystal supplies us with the possibility to investigate the effect of pressure on tautomeric equilibrium.

**Dynamic Switching Behavior of OX-1 under High Pressure.** To study the effect of pressure on molecular tautomerization of OX-1, the sample was put in a diamond

anvil cell (DAC) equipment, which can generate hydrostatic pressure with dozens of gigapascals at room temperature. As shown in Figure 3a, the crystal of OX-1 is pale yellow with good optical transparency under ambient pressure. When the external pressure was gradually increased from 0 to 10 GPa, the color of the crystal underwent a continuous and remarkable variation from pale yellow to orange to red, and finally to dark red. Correspondingly, in situ UV-vis absorption spectra clearly revealed that the absorption of crystal OX-1 shifted and broadened continuously to longer wavelength, demonstrating a marvelous pressure-tunable absorption across nearly the entire visible light region (from ~430 to ~700 nm) (Figure 3b), and it has been proven that the absorption spectra will not change with the prolonging of time at each tested pressure points, which means the equilibrium is reached right after the pressure is stabilized (Supporting Information Figure S10). This amazing optical modulation indicates that multiple optical states are generated in the simple bistate molecular switch of OX-1 with the only stimulus of pressure. The phenomenon has distinct difference with light-triggered tautomerization, which only results in the appearing of a new absorption peak (Figure 2b and Supporting Information Figure S3a). The in situ Raman spectra of OX-1 provide an opportunity to monitor the molecular structure change with increasing pressure and understand the absorption/color change. It is found that the Raman spectra in the wavenumber range of 50–1300 cm<sup>-1</sup> are too weak to be reliably used for analysis, owing to the strong fluorescent interference (Supporting Information Figure S7).

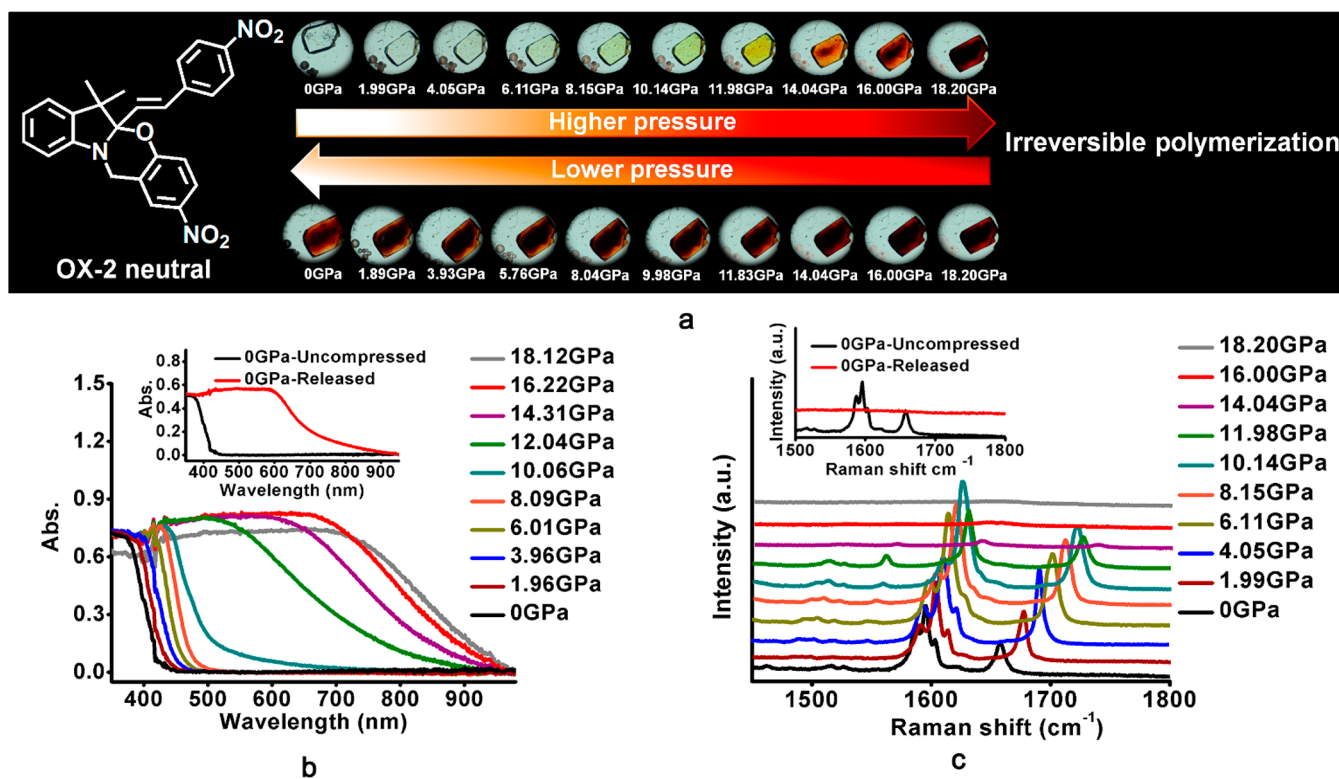


**Figure 4.** Molecular structure of OX-2 in neutral forms, and real optical images of an OX-2 crystal with increasing and decreasing pressure (a) (the balls at bottom left corner in DAC are ruby pressure markers). In-situ absorption (b) and Raman (c) spectra of the OX-2 crystal in the DAC with increasing pressure (inset: comparison of the absorption and Raman spectra of OX-2 in the uncompressed and released states).

Fortunately, its Raman spectra in the wavenumber range of 1400–1800  $\text{cm}^{-1}$  are clear enough to track the molecular structure change (Figure 3c). Before compression, there are two sets of Raman peaks (black line in Figure 3c). According to the calculation results with B3LYP/6-31+G (d,p)<sup>38</sup> (Supporting Information Figure S8 and Video 1), the first set consists of the two strong peaks at 1608 and 1647  $\text{cm}^{-1}$ , which are assigned to the two different vibration modes of isolated  $\pi$ -system of *N,N*-dimethyl-4-vinyl benzenamine of neutral isomer (black arrow in Figure 3c); the second set consists of the peaks around 1608, 1540, and 1480  $\text{cm}^{-1}$ , which corresponds to the extended conjugated  $\pi$ -systems of cyanine and nitrophenolate of the zwitterionic isomer (red arrow in Figure 3c). This result is also in agreement with our aforesaid assessment that the tautomerization is a dynamic equilibrium in its crystal state and the neutral isomer is thermodynamically favorable under ambient pressure. When external pressure was applied, both sets of Raman peaks shifted slowly toward higher frequencies as a result of the shortening in interatomic distances and strengthening in the effective force constants.<sup>39,40</sup> In the meantime, their relative peak intensities of zwitterionic isomer to neutral isomer increased gradually with pressure, indicating external compression have definitely changed the tautomerization equilibrium. The rough estimation based on the Raman spectra shows that the proportion of zwitterionic isomers increases from 8% to 83% during the compression (Supporting Information Figure S9).

When pressure was removed gradually, both absorption and Raman spectra of OX-2 recovered concomitantly (Supporting Information Figure S11 and S12). However, there are some edges in which the red color does not fade completely in the microscopy images (Figure 3a), suggesting that some irreversible alterations on molecular arrangements or conformations occur as

a result of the anisotropic deformation on these edges. Because the portions of the edges are not much, it did not result in a significant change in absorption and Raman spectra (Figure 3b and c inset). Therefore, benzo[1,3]oxazine OX-1 is a good candidate for pressure-controllable dynamic molecular switch. Although some spiropyrans have been demonstrated to be switched by stretching or shearing their polymer blends,<sup>41–46</sup> these processes are usually irreversible. Bonds breaking by stretching or shearing is understandable; however, the compression-induced bond breaking is uncommon and will be discussed later.

**Performances of OX-2 under High Pressure.** The exciting pressure-tunable dynamic switching process has been observed in the crystal of OX-1, and continuous optical states can be built by shifting its tautomerization equilibrium with pressure. Though OX-2 does not exhibit stable zwitterionic isomers in solution or crystal states without external stimuli, pressure is a powerful tool to shorten intermolecular distance to change intermolecular interactions and molecular internal energy, which might give rise to significant effects on the tautomerization of OX-2 in crystal. To test our hypothesis, we investigate the high pressure behavior of OX-2. However, a distinctly different phenomenon is observed (Figure 4). In the pressure range of 0 to 10 GPa, the crystal of OX-2 exhibits much smaller absorption spectral change (from  $\sim 400$  nm to  $\sim 480$  nm) (Figure 4b) and limited color change from colorless to yellow (Figure 4a). Although the absorption peak of zwitterionic isomer of OX-2 is around 400 nm with a pale yellow color in solution (Figure 2c), the spectra change for OX-2 at 10 GPa is concluded not to originate from its zwitterionic isomers but from enhanced intermolecular interactions because their Raman spectra only shows a common shift to high frequencies without any detectable

new peaks (Figure 4c). The detailed analysis on main Raman peaks' shifts as a function of pressure shows that the main peaks of OX-2 have good linear relationships with pressure, which indicates that there are not any chemical transitions involved during this compressed process (0–10 GPa) (Supporting Information Figure S13).

When pressure reaches 12 GPa, an abrupt color and absorption spectra change for OX-2 occurs (Figure 4a and 4b). Thereafter, the color of crystal OX-2 continuously deepens and finally turns to reddish dark in the middle part of the crystal (Figure 4a) with its absorption shifting to around 800 nm (Figure 4b). Meanwhile, the Raman spectra gradually vanishes when pressure is further increased to 18 GPa (Figure 4c), which is a result of strong background inference of fluorescence. More interestingly, the color, absorption, and Raman spectra of OX-2 could not recover after the pressure is totally removed (Figure 4). Further detailed investigation reveals that the OX-2 crystal can be fully restored to its original state when the pressure reaches only 10 GPa (Supporting Information Figure S14), and most of it can recover when the pressure reaches 12 GPa. But when pressure reaches 14 GPa, the compressed OX-2 cannot recover, especially for the Raman spectra, which completely disappears when the pressure is released (Supporting Information Figure S15). The phenomenon indicates that an irreversible chemical reaction takes place between 10 and 12 GPa range and only physical compression with good reversibility is involved before 10 GPa. This irreversible chemical reaction of OX-2 under high pressure inspires us to investigate whether a similar irreversible chemical transition also takes place in OX-1 crystal at higher pressure. To answer this question, we further compressed the OX-1 crystal to 18 GPa from 10 GPa. As anticipated, when pressure was removed, the color of OX-1 crystal remained black, and the absorption and Raman spectra also could not recover to the original state (Supporting Information Figure S16), which indicates that OX-1 also undergoes an irreversible chemical reaction when pressure is high enough.

These irreversible reactions for OX-1 and OX-2 maybe come from the polymerization of parallel aromatic rings. It has been demonstrated that the polymerization of benzene will be triggered when C···C distance between adjacent benzene rings reach the critical threshold of 2.6 Å.<sup>47</sup> In the crystal OX-1 and OX-2, the distances of their  $\pi\cdots\pi$  interactions are 3.991 and 3.386 Å (or 3.864 Å) (Figure 1), respectively, which provides a possibility for the polymerization of aromatic rings under pressure. In addition, the polymerization of benzene involves the ring-opening of the benzene ring and transforms an  $sp^2$  carbon atom into an  $sp^3$  atom.<sup>48</sup> Comparing with uncompressed samples of OX-1 and OX-2, the relative peak intensities of the saturated C–H to aromatic ring in highly compressed and irreversible crystals obviously increase (Supporting Information Figure S17), which further suggests that the irreversible chemical reactions are originated from the polymerization of the parallel aromatic rings. To sum up, both OX-1 and OX-2 can undergo irreversible chemical transformation when they are highly compressed. But for OX-1, it shows pressure-controllable and reversible tautomerization in the low pressure range (0–10 GPa). However, OX-2 does not exhibit the tunable tautomeric equilibrium under compression like OX-1, it only shows pressure-tunable reversible configuration change at low pressure (0–10 GPa) and an irreversible polymerization at high pressure.

**Understanding the Different High-Pressure Behavior of OX-1 and OX-2.** In the above two sections, it is shown that two benzo[1,3]oxazine analogues of OX-1 and OX-2 exhibit

remarkably different high-pressure responses. For OX-1, pressure can significantly change tautomerization equilibrium. But for OX-2, pressure cannot lead to the tautomerization until irreversible polymerization occurs. Thus, it is very necessary to understand in what circumstance pressure can affect the tautomerization and why pressure can shift the tautomerization equilibrium. Quite different from stretching or shearing induced bond breakage of molecular switches in polymers, hydrostatic pressure leads to the shrinkage in the volume of crystals. Thus, it can be deduced that the isomer with smaller occupied volume will be favored under pressure. We first calculate the molecular volumes of OX-1 in neutral and zwitterionic forms by B3LYP/6-31+G (d,p) calculations<sup>38</sup> in a vacuum (Supporting Information Figure S4). The optimized molecular volume of zwitterionic isomer of OX-1 is a little larger than that of optimized neutral isomer (374.610 vs 338.652  $\text{cm}^3\cdot\text{mol}^{-1}$ ) because the nitrophenolate group tends to rotate around the C–N bond after the cleavage of C–O bond in vacuum (Supporting Information Figure S4). From the viewpoint of volume variation, the compression process seems not to be favorable for the zwitterionic ring-open isomer of OX-1. But in fact, in the constraint crystal, especially in a highly compressed state, the rotation of the C–N bond should not easily take place. Here, we are inclined to think that the phenol oxygen atom in zwitterionic isomer of OX-1 is not much deviated from the original position in its neutral isomer under isotropic hydrostatic pressure, which is directly deduced from the evidence that the neutral isomer can restore immediately when pressure is removed. To test our deduction, we utilize another stimulus of mechanical grinding to trigger the tautomerization. The grinding-induced zwitterionic isomer of OX-1 could stand well for one year under ambient conditions, and it could not recover to its original state even when it is heated at 100 °C for 20 min (Supporting Information Figure S18). This poor reversibility in grinding-induced tautomerization of OX-1 is just attributed to a large deviation of the nitrophenolate from its original position caused by the anisotropic stress-triggered configurational or conformational variation, and it is difficult for the rebuilding of C–O bond. Though the molecular volumes of neutral and zwitterionic isomers do not exhibit significant differences under compression, the compressibility of two isomers is quite different. Compared with the relatively rigid cyclized framework of the neutral isomer, the nitrophenolate fragment in the zwitterionic isomer is more flexible and compressible, which might be a main driven force for the pressure-tunable tautomerization of OX-1. In the meantime, the resultant cyanine structure in the zwitterionic isomer would be more planar than before, which also favors its high compressibility.

Besides the compressibility, we can understand the pressure-shifted tautomerization from the viewpoint of molecular energy. Under ambient pressure, the energy differences between the zwitterionic and neutral isomers are 9.17  $\text{kcal}\cdot\text{mol}^{-1}$  and 18.28  $\text{kcal}\cdot\text{mol}^{-1}$  in vacuum for OX-1 and OX-2, respectively, according to theoretical calculations (Supporting Information Figure S4 and S5). That means the neutral isomers are dominant components for both OX-1 and OX-2 without pressure. During the shrinkage of crystal volume under pressure, the molecular energies will be boosted to higher levels by increasing the molecular tension. Due to the better compressibility and stronger intermolecular interactions between zwitterionic isomers, the energy rise of zwitterionic isomer should not be as much as that of a neutral isomer with increasing pressure. As a result, an inversion of the relative energy levels distribution between two

isomers might take place for OX-1 owing to their relatively small energy difference (Supporting Information Figure S4), and the zwitterionic isomers of OX-1 with lower energy under high pressure might be more favorable (Figure 5a). The low

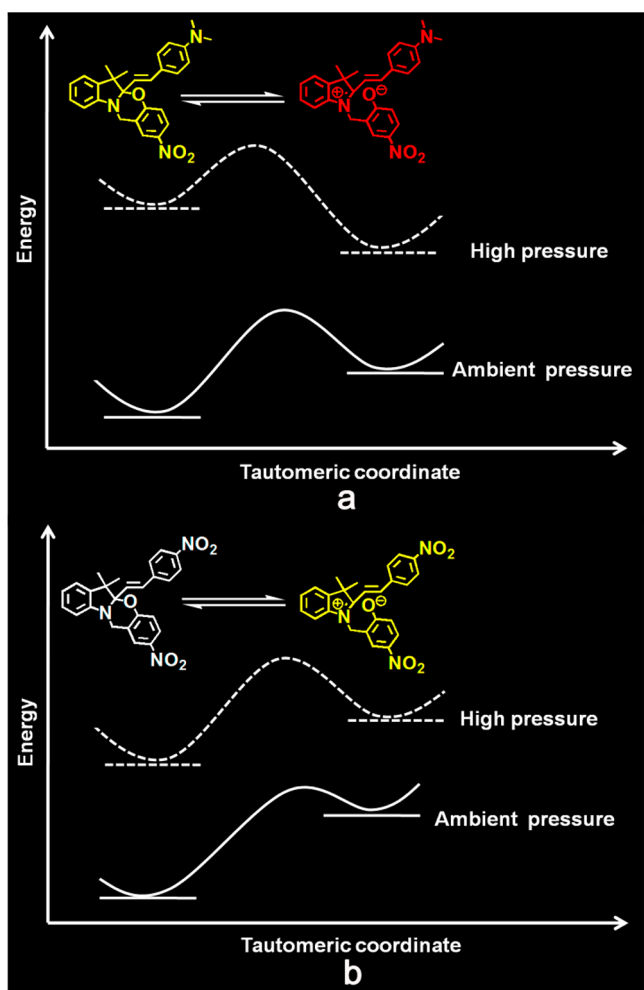


**Figure 5.** Potential energy diagram for the tautomeric equilibria of OX-1 (a) and OX-2 (b) under different conditions.

tautomerization energy barrier ( $\Delta G = 11.51 \text{ kcal}\cdot\text{mol}^{-1}$ ) enable the heterocleavage of the C–O bond happen at room temperature and shift the tautomeric equilibrium of OX-1 toward zwitterionic isomers. In addition, as mentioned above, zwitterionic isomer of OX-1 is more favorable in polar environment in solution (Figure 2d). In a crystal, the zwitterionic isomer with much larger dipole moment than that of neutral one (Supporting Information Figure S4), which can supply the polar environments. When pressure drives the tautomeric equilibrium of OX-1 to generate more zwitterionic isomers, a more polar microenvironment is also formed. In return, it will help to stabilize the newly generated zwitterionic isomers under high pressure. Therefore, a better compressibility of the zwitterionic isomer, the smaller energy gap and the inversion of the relative energy levels between the two isomers, the more polar microenvironment under high pressure, and low tautomerization energy barrier together contribute to the pressure-controllable dynamic switching of OX-1 in crystal.

For OX-2, the molecular energies between two isomers are also elevated with increasing pressure. However, on the one hand, the inversion of the relative energy levels distribution

between two isomers should be harder to occur under moderate compression (0–10 GPa) owing to the high energy differences between two isomers (Supporting Information Figure S5). On the other hand, the large tautomerization energy barrier ( $16.86 \text{ kcal}\cdot\text{mol}^{-1}$ ) (Supporting Information Table S1) makes the tautomerization hard to happen at room temperature (Figure 5b). When pressure is further increased, the irreversible polymerization is triggered. Therefore, we can conclude that the lower tautomerization barrier and smaller energy gap between the isomers of molecular switches are preliminary requirements for the pressure-tunable tautomerization process.

Considering the fact that light-stimulus can induce the tautomerization of OX-1 and OX-2 in both solution and solid states, we can clearly find that the effects of two energy inputs (light and pressure) on the molecular tautomerization are quite different. For light-stimulated tautomerization, the light can be absorbed by the neutral molecule in both free and restricted states to excite their electron from ground-state to excited-state, which then polarizes the molecule and result in the cleavage of the weak C–O bond to generate zwitterionic isomer. In other words, the energy of the neutral molecule is boosted by absorbing the light energy, and then it overcomes the energy barrier to reach the zwitterionic states. A static UV–vis absorption change can be detected as long as the zwitterionic isomer can be stabilized in its microenvironment, otherwise, it will revert to the neutral isomer instantly.<sup>19</sup> For pressure stimulus, it cannot excite the electron of the molecule to its excited-state, but instead, it can change the energy of the molecule by strengthening intermolecular interactions in the restricted state (e.g., crystal state). As a result, the distribution of the relative energy levels of the neutral isomer, the zwitterionic isomer and the transition state may change with their different susceptibility to pressure. However, it can only absorb ambient heat to overcome the energy barrier; therefore, it is difficult to apply only pressure to induce the tautomerization for molecules that have high tautomeric energy barriers (e.g., OX-2).

**Understanding the Continuous, Large-Scale, and Reversible Optical Modulation under Pressure and the Application Potentials.** Though the bathochromic shift in absorption spectra of electronic transition with increasing pressure has been observed in some organic crystals, polymers, and metal complexes,<sup>49–51</sup> the continuously shifting and broadening of spectra covering nearly the entire visible region (from  $\sim 430$  to  $\sim 700$  nm) for OX-1 are still unusual. For common polymers or some conjugated organic molecules, pressure-induced better planarity and strengthened overlap of  $\pi$ -electrons by shortening intermolecular distance are responsible for the bathochromic shift in the absorption (around 100 nm).<sup>52–55</sup> For OX-1, besides the better planarity and enhanced intermolecular interactions, we think that the molecular structural transformation contributes more to the large-scale spectra bathochromic shift. To confirm this assumption, we investigated another single crystal of IA-1, which has an analogous conjugated structure with zwitterionic OX-1 but lacks structural adjustability (Figure 1 and Supporting Information Figure S19a). During the compression, an obvious red-shift in its absorption spectra is observed at the pressure around 1 GPa. This could be assigned to pressure-induced molecular planarity. When pressure is further increased to 10 GPa, its absorption spectra exhibit sequentially bathochromic shift like common organic compounds and accompany with a color change from pale yellow to orange (Supporting Information Figure S19a and S19b). But its absorption shifts

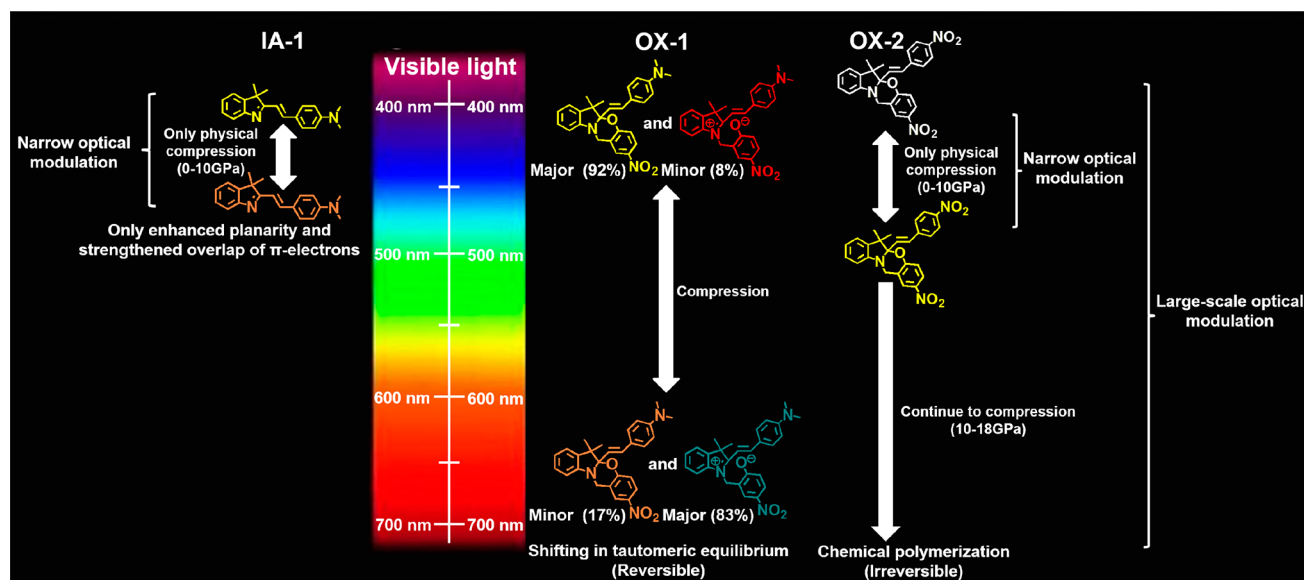


Figure 6. Illustration of different optical modulations of IA-1, OX-1, and OX-2 under pressure.

only around 40 nm, which indicates that a simple conjugated system shows limited bathochromic shift in the absorption spectra (Figure 6). Moreover, in the range of 0–10 GPa, the absorption wavelength of OX-2 also shifts only 70 nm (Figure 4b and Supporting Information Figure S14). Therefore, without chemical structure tautomerization, pressure-induced better planarity and strengthened overlap of  $\pi$ -electrons can only give rise to narrow optical modulation in conjugated organic crystals. Nevertheless, the simple physical compression usually exhibits good reversibility. But when the threshold pressure for chemical reaction reaches, an irreversible polymerization is triggered in the OX-2 crystal. As a result, an abrupt and obvious spectra shift (around 100 nm) is observed. Also, with the going of the chemical reaction, the absorption spectra of OX-2 bathochromically shift to around 800 nm and cover almost entire visible region (Figure 4b). Based on the above discussions, we can find that chemical transition in crystal plays an important role on the large-scale optical modulation. But for reversible and large-scale optical modulator, the irreversible polymerization mode (such as OX-2) is not ideal (Figure 6).

The continuous, large-scale, and reversible optical modulation of OX-1 in crystal can be ascribed to its pressure-controllable tautomerization before reaching the threshold pressure of irreversible chemical reaction. Under ambient pressure, the neutral and zwitterionic isomers of OX-1 coexist in crystal with absorption maximums at 426 and 574 nm, respectively (Supporting Information Figure S2), which means that OX-1 has two different compression starts (with  $\sim 150$  nm gaps). When OX-1 is compressed, external pressure shortens intermolecular distance to drive the absorptions of two isomers bathochromic shift from their different starts. In addition, the ratio of two isomers is variable with increasing pressure. In this way, the two coexisting isomers of OX-1 with pressure-tunable ratios and bathochromic shift degree finally result in the large-scale optical modulation. At the same time, the tautomerization of OX-1 between two isomers is strictly pressure dependent. Thus, its optical modulation is well reversible (Figure 6 and Supporting Information Video 2).

The above demonstrated novel pressure-controlled, large-scale structural adaption to pressure for OX-1 will undoubtedly

induce its physical property changes (such as light absorption, dielectric constant, conductivity, etc.) and bring about new applications for molecular switches, such as large-scale optical modulation materials, energy storage materials, pressures sensors, and so on. However, we do not have the facility so far to measure all these properties. Here, as an example, we show the application potentials of OX-1 as both a rough visible pressure indicator and a relatively accurate pressure sensor. As we can see in Figure 3a, the color change at every 1 GPa pressure increment can be clearly distinguished, which endorses OX-1 as a good candidate for a convenient and rough colorimetric pressure indicator just like pH test strips. What's more, the Raman peak's shift at  $1608\text{ cm}^{-1}$  is linear with pressure (Figure 7), which provides another opportunity for OX-1 to sense pressure more precisely. Most importantly, the process is reversible, after three cycles of compressions and decompressions, the Raman spectra of OX-1 could still revert to the original state (Figure 7 inset). The good reversibility would be of benefit to its practical application. We expect that new properties and applications will

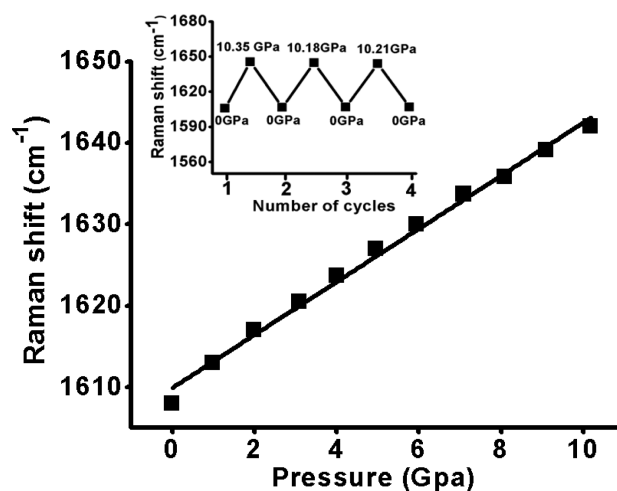
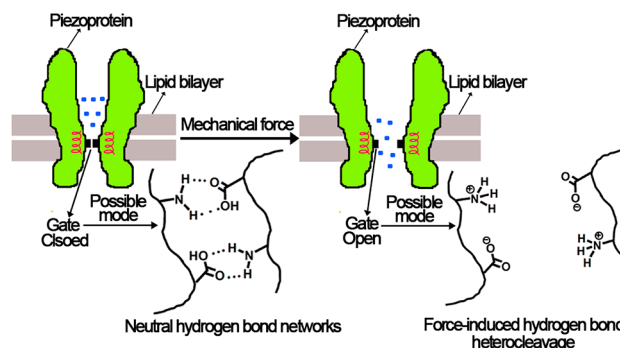


Figure 7. Shift of the Raman peak at  $1608\text{ cm}^{-1}$  of OX-1 with pressure (inset: peak values of OX-1 at  $1608\text{ cm}^{-1}$  under three cycles of compression and decompression).

be further explored for molecular switches where research facilities allow.

**Reflection of the Pressure-Controlled Molecular Tautomerization on Tactile Sensing.** As we stress in the beginning of the paper, developing pressure-responsive molecular switches is on the one hand for the development of novel functional materials, and on the other hand for understanding the tactile sensation mechanism of biological system. It is well known that the key of tactile sensing is transforming a mechanical signal into an electrical signal, in which external mechanical stimuli induce the ion channels to open and finally generate the electrical signal. However, we have little knowledge on how mechanical force induces the ion channels to open. Although some piezoproteins have been revealed to be related to the mechanotransduction, the working mechanisms of the mechanoreceptors are still unclear.<sup>56,57</sup> Our research results here show the following two facts: (1) even in confined solid state, dynamic molecular tautomerization (reversible bond heterocleavage) are still possible at room temperature and (2) external pressure can shift the tautomerization equilibrium by changing the relative energy levels of the two isomers, transforming the “less polar” neutral isomers to the “highly polarized” zwitterionic isomers. In this way, the molecular switches work as a nanopiezoelectric machine, transforming the mechanical energy to electric potential. Because the mechanotransduction process also relies on the mechanical-to-electrical signal transition in a tactile nerve, we propose that one possible path of mechanotransduction is also rely on the reversible bond heterocleavage.

Choosing from the amino acid library, we think it is unlikely that the less polar covalent bond will be broken in a protein to result in zwitterionic forms. However, the ubiquitous supramolecular bonds can be easier to break and result in polarized zwitterionic species by heterocleavage. Also, we suggest one of the most probable supramolecular bond is the polar hydrogen bond between the acidic groups (e.g., carboxylic acid, phenol) and basic groups (e.g., amino, imidazolyl) in the proteins. The interaction modes between the acidic and basic groups can vary with their  $pK_a$  and  $pK_b$  depending on their associated structures and microenvironment. If the acidity of the acidic group is not strong enough to protonate the basic group, they can form neutral supramolecules by hydrogen bonds; conversely, zwitterions of carboxylate anion and ammonium cation are generated. The  $pK_a$  and  $pK_b$  of the amino acid are constants at a certain temperature in solution. However, our results show that force can trigger the molecular reaction that does not dominate at ambient pressure to occur at higher pressure by increasing the molecular interactions in solid state. Our previous study also elucidates that the molecular acidity of a conjugated amphoteric molecules can also be enhanced with mechanical force, and a proton transfer is triggered subsequently.<sup>58</sup> Although we cannot give the details of how molecular acidity and basicity in protein can be modified by intermolecular interaction under mechanical force so far, we strongly believe that proton transfer between the neutral acid–base pair in protein is possible under a mechanical trigger; as a result, the neutral to ionic state transformation will lead to the closed ion channel to open and realize the mechanotransduction (Figure 8). Our next focus will be concentrated on developing other dynamic mechanoresponsive small molecular systems and shine further light on tactile sensing mechanism. In the meantime, computational modeling will be carried out in proteins to test the possibilities of proton transfer in our proposed model.



**Figure 8.** Possible working mechanism of piezoprotein in tactile sensing system.

## CONCLUSIONS

In summary, we have presented a pioneered pressure-controllable molecular switch of OX-1, which realizes the bistable state to continuous state transition in a crystal by pressure-enhanced intermolecular interactions. When pressure increases from 0 to 10 GPa, a continuous and reversible large-scale absorption modulation across the whole visible light range (from ~430 to ~700 nm) is realized. The pressure-controllable molecular tautomerization is found to be related to its low tautomeric energy barrier of tautomerization, the small energy gap between the two isomers, and the strong environmental sensitivity of the tautomerization equilibrium. In contrast, the relatively high tautomeric energy barrier, and weak environmental sensitivity of the tautomerization equilibrium make OX-2 lack of a dynamic switching behavior in crystal. The molecular tautomerization ratio increment from the original 8% to 83% for OX-1 is found to contribute more to the large-scale optical modulation than the configuration change. This novel reversible pressure-dependent color and Raman shift show the application potential in pressure sensors. Results from our experiments not only enrich the understanding on the dynamic structural tautomerization in crystal and the adaption of molecular structure to microenvironments but also inspire us to propose a possible model of hydrogen-bond heterocleavage for mechanotransduction in tactile sensing.

## ASSOCIATED CONTENT

### Supporting Information

Detailed experimental procedures and characterization data for the OX-1, OX-2, and IA-1. This material is available free of charge via the Internet at <http://pubs.acs.org>.

## AUTHOR INFORMATION

### Corresponding Authors

\*liminjie@jlu.edu.cn

\*zoubo@jlu.edu.cn

\*seanzhang@jlu.edu.cn

### Notes

The authors declare no competing financial interest.

## ACKNOWLEDGMENTS

The authors acknowledge Prof. Bingbing Liu for IR spectra measurements and Prof. Bing Zhao for discussion on Raman spectra. We thank NSFC (51373068 and 91227202) and the program of Chang Jiang Scholars and Innovative Research Team in University (IRT101713018) for financial support.



## REFERENCES

- (1) Godsi, O.; Peskin, U.; Kapon, M.; Natan, E.; Eichen, Y. *Chem. Commun.* **2001**, 2132–2133.
- (2) Berkovic, G.; Krongauz, V.; Weiss, V. *Chem. Rev.* **2000**, *100*, 1741–1753.
- (3) Minkin, V. I. *Chem. Rev.* **2004**, *104*, 2751–2776.
- (4) Natansohn, A.; Rochon, P. *Chem. Rev.* **2002**, *102*, 4139–4175.
- (5) Irie, M. *Chem. Rev.* **2000**, *100*, 1685–1716.
- (6) Zhu, M. Q.; Zhang, G. F.; Li, C.; Aldred, M. P.; Chang, E.; Drezek, R. A.; Li, A. D. Q. *J. Am. Chem. Soc.* **2011**, *133*, 365–372.
- (7) Tian, Z.; Wu, W.; Wan, W.; Li, A. D. Q. *J. Am. Chem. Soc.* **2011**, *133*, 16092–16100.
- (8) Yam, V. W. W.; Lee, J. K. W.; Ko, C. C.; Zhu, N. J. *Am. Chem. Soc.* **2009**, *131*, 912–913.
- (9) Poon, C. T.; Lam, W. H.; Wong, H. L.; Yam, V. W. W. *J. Am. Chem. Soc.* **2010**, *132*, 13992–13993.
- (10) Kawata, S.; Kawata, Y. *Chem. Rev.* **2000**, *100*, 1777–1788.
- (11) Szacilowski, K. *Chem. Rev.* **2008**, *108*, 3481–3548.
- (12) Li, K.; Xiang, Y.; Wang, X.; Li, J.; Hu, R.; Tong, A.; Tang, B. Z. *J. Am. Chem. Soc.* **2014**, *136*, 1643–1649.
- (13) Raymo, F. M.; Alvarado, R. J.; Giordani, S.; Cejas, M. A. *J. Am. Chem. Soc.* **2003**, *125*, 2361–2364.
- (14) Jiang, G.; Song, Y.; Guo, X.; Zhang, D.; Zhu, D. *Adv. Mater.* **2008**, *20*, 2888–2898.
- (15) Tian, H.; Yang, S. *Chem. Soc. Rev.* **2004**, *33*, 85–97.
- (16) Tan, W.; Zhang, Q.; Zhang, J.; Tian, H. *Org. Lett.* **2009**, *11*, 161–164.
- (17) Bénard, S.; Yu, P. *Chem. Commun.* **2000**, 65–66.
- (18) Patel, D. G.; Benedict, J. B.; Kopelman, R. A.; Frank, N. L. *Chem. Commun.* **2005**, 2208–2210.
- (19) Harada, J.; Kawazoe, Y.; Ogawa, K. *Chem. Commun.* **2010**, 46, 2593–2595.
- (20) Sheth, A. R.; Lubach, J. W.; Munson, E. J.; Muller, F. X.; Grant, D. J. W. *J. Am. Chem. Soc.* **2005**, *127*, 6641–6651.
- (21) Schettino, V.; Bini, R. *Phys. Chem. Chem. Phys.* **2003**, *5*, 1951–1965.
- (22) Kaupp, G. *CrystEngComm* **2009**, *11*, 388–403.
- (23) Baig, R. B. N.; Varma, R. S. *Chem. Soc. Rev.* **2012**, *41*, 1559–1584.
- (24) Ariga, K.; Mori, T.; Hill, J. P. *Adv. Mater.* **2012**, *24*, 158–176.
- (25) Jezowski, S. R.; Zhu, L.; Wang, Y.; Rice, A. P.; Scott, G. W.; Bardeen, C. J.; Chronister, E. L. *J. Am. Chem. Soc.* **2012**, *134*, 7459–7466.
- (26) Tomasulo, M.; Sortino, S.; Raymo, F. M. *Org. Lett.* **2005**, *7*, 1109–1112.
- (27) Tomasulo, M.; Sortino, S.; White, A. J. P.; Raymo, F. M. *J. Org. Chem.* **2005**, *70*, 8180–8189.
- (28) Tomasulo, M.; Sortino, S.; Raymo, F. M. *Adv. Mater.* **2008**, *20*, 832–835.
- (29) Tomasulo, M.; Deniz, E.; Benelli, T.; Sortino, S.; Raymo, F. M. *Adv. Funct. Mater.* **2009**, *19*, 3956–3961.
- (30) Tomasulo, M.; Raymo, F. M. *J. Mater. Chem.* **2005**, *15*, 4354–4360.
- (31) Prostota, Y.; Berthet, J.; Delbaere, S.; Coelho, P. J. *Dyes Pigm.* **2013**, *96*, 569–573.
- (32) Deniz, E.; Tomasulo, M.; Sortino, S.; Raymo, F. M. *J. Phys. Chem. C* **2009**, *113*, 8491–8497.
- (33) Deniz, E.; Ray, S.; Tomasulo, M.; Impellizzeri, S.; Sortino, S.; Raymo, F. M. *J. Phys. Chem. A* **2010**, *114*, 11567–11575.
- (34) Cusido, J.; Battal, M.; Deniz, E.; Yildiz, I.; Sortino, S.; Raymo, F. M. *Chem.—Eur. J.* **2012**, *18*, 10399–10407.
- (35) Zhu, S.; Li, M.; Sheng, L.; Chen, P.; Zhang, Y.; Zhang, S. X. -A. *Analyst* **2012**, *137*, 5581–5585.
- (36) Xie, X.; Crespo, G. A.; Bakker, E. *Anal. Chem.* **2013**, *85*, 7434–7440.
- (37) Zhu, S.; Li, M.; Zhang, Y.; Tang, S.; Yang, J.; Wang, Y.; Sun, L.; Sheng, L.; Yang, B.; Zhang, S. X. -A. *RSC Adv.* **2013**, *3*, 19752–19755.
- (38) Frisch, M. J.; Trucks, G. W.; Schlegel, H. B.; Scuseria, G. E.; Robb, M. A.; Cheeseman, J. R.; Scalmani, G.; Barone, V.; Mennucci, B.; Petersson, G. A.; Nakatsuji, H.; Caricato, M.; Li, X.; Hratchian, H. P.; Izmaylov, A. F.; Bloino, J.; Zheng, G.; Sonnenberg, J. L.; Hada, M.; Ehara, M.; Toyota, K.; Fukuda, R.; Hasegawa, J.; Ishida, M.; Nakajima, T.; Honda, Y.; Kitao, O.; Nakai, H.; Vreven, T.; Montgomery, J.; Peralta, J. E.; Ogliaro, F.; Bearpark, M.; Heyd, J. J.; Brothers, E.; Kudin, K. N.; Staroverov, V. N.; Kobayashi, R.; Normand, J.; Raghavachari, K.; Rendell, A.; Burant, J. C.; Iyengar, S. S.; Tomasi, J.; Cossi, M.; Rega, N.; Millam, J. M.; Klene, M.; Knox, J. E.; Cross, J. B.; Bakken, V.; Adamo, C.; Jaramillo, J.; Gomperts, R.; Stratmann, R. E.; Yazyev, O.; Austin, A. J.; Cammi, R.; Pomelli, C.; Ochterski, J. W.; Martin, R. L.; Morokuma, K.; Zakrzewski, V. G.; Voth, G. A.; Salvador, P.; Dannenberg, J. J.; Dapprich, S.; Daniels, A. D.; Farkas, O.; Foresman, J. B.; Ortiz, J. V.; Cioslowski, J.; Fox, D. J. *Gaussian 09*, Revision A.01; Gaussian, Inc.: Wallingford, CT, 2009.
- (39) Wang, K.; Duan, D.; Wang, R.; Lin, A.; Cui, Q.; Liu, B.; Cui, T.; Zou, B.; Zhang, X.; Hu, J.; Zou, G.; Mao, H. K. *Langmuir* **2009**, *25*, 4787–4791.
- (40) Tan, X.; Wang, K.; Li, S.; Yuan, H.; Yan, T.; Liu, J.; Yang, K.; Liu, B.; Zou, G.; Zou, B. *J. Phys. Chem. B* **2012**, *116*, 14441–14450.
- (41) Davis, D. A.; Hamilton, A.; Yang, J.; Cremer, L. D.; Gough, D. V.; Potisek, S. L.; Ong, M. T.; Braun, P. V.; Martínez, T. J.; White, S. R.; Moore, J. S.; Sottos, N. R. *Nature* **2009**, *459*, 68–72.
- (42) Lee, C. K.; Davis, D. A.; White, S. R.; Moore, J. S.; Sottos, N. R.; Braun, P. V. *J. Am. Chem. Soc.* **2010**, *132*, 16107–16111.
- (43) Kingsbury, C. M.; May, P. A.; Davis, D. A.; White, S. R.; Moore, J. S.; Sottos, N. R. *J. Mater. Chem.* **2011**, *21*, 8381–8388.
- (44) Beiermann, B. A.; Kramer, S. L. B.; Moore, J. S.; White, S. R.; Sottos, N. R. *ACS Macro Lett.* **2012**, *1*, 163–166.
- (45) Grady, M. E.; Beiermann, B. A.; Moore, J. S.; Sottos, N. R. *ACS Appl. Mater. Interfaces* **2014**, *6*, 5350–5355.
- (46) Beiermann, B. A.; Kramer, S. L. B.; May, P. A.; Moore, J. S.; White, S. R.; Sottos, N. R. *Adv. Funct. Mater.* **2014**, *24*, 1529–1537.
- (47) Ciabini, L.; Santoro, M.; Gorelli, F. A.; Bini, R.; Schettino, V.; Raugei, S. *Nat. Mater.* **2007**, *6*, 39–43.
- (48) Ciabini, L.; Santoro, M.; Bini, R.; Schettino, V. *J. Chem. Phys.* **2002**, *116*, 2928–2935.
- (49) Taran, M. N.; Langer, K.; Koch-Müller, M. *Phys. Chem. Miner.* **2008**, *35*, 175–177.
- (50) Byrne, P. J.; Richardson, P. J.; Chang, J.; Kusmartseva, A. F.; Allan, D. R.; Jones, A. C.; Kamenev, K. V.; Tasker, P. A.; Parsons, S. *Chem.—Eur. J.* **2012**, *18*, 7738–7748.
- (51) Fanetti, S.; Citroni, M.; Malavasi, L.; Artioli, G. A.; Postorino, P.; Bini, R. *J. Phys. Chem. C* **2013**, *117*, 5343–5351.
- (52) Shirovani, I.; Hayashi, J.; Takeda, K.; Kawamura, H.; Inokuchi, M.; Yakushi, K.; Inokuchi, H. *Mol. Cryst. Liq. Cryst.* **2007**, *461*, 111–122.
- (53) Chandrasekhar, M.; Guha, S.; Graupner, W. *Adv. Mater.* **2001**, *13*, 613–618.
- (54) Webster, S.; Batchelder, D. N. *Polymer* **1996**, *37*, 4961–4968.
- (55) Shirovani, I. *Platinum Met. Rev.* **1987**, *31*, 20–23.
- (56) Coste, B.; Mathur, J.; Schmidt, M.; Earley, T. J.; Ranade, S.; Petrus, M. J.; Dubin, A. E.; Patapoutian, A. *Science* **2010**, *330*, 55–60.
- (57) Roudaut, Y.; Lonigro, A.; Coste, B.; Hao, J.; Delmas, P.; Crest, M. *Channels* **2012**, *6*, 234–245.
- (58) Wang, Y.; Li, M.; Zhang, Y.-M.; Yang, J.; Zhu, S.; Sheng, L.; Wang, X.; Yang, B.; Zhang, S. X. -A. *Chem. Commun.* **2013**, *49*, 6587–6589.